

with that of high-latitude ice cores may reflect a nonlinear threshold response in atmospheric circulation patterns or in the hydrologic system at this maritime mid-latitude site. The rapid return to baseline trace element values in stalagmite CC3 at  $8310 \pm 80$  years B.P. is consistent with a rapid reestablishment of North Atlantic THC (20) ending the cold, dry episode in Ireland.

#### References and Notes

- W. Dansgaard *et al.*, *Nature* **364**, 218 (1993).
- P. M. Grootes, M. Stuiver, J. W. C. White, S. J. Johnsen, J. Jouzel, *Nature* **366**, 552 (1993).
- G. Bond *et al.*, *Science* **278**, 1257 (1997).
- D. Klitgaard-Kristensen, H. P. Sejrup, H. Hafflidson, S. Johnsen, M. Spurk, *J. Quat. Sci.* **13**, 165 (1998).
- D. R. Rousseau, R. Prece, N. Limondin-Lozouet, *Geology* **26**, 651 (1998).
- U. von Grafenstein, H. Erlenkeuser, J. Muller, J. Jouzel, S. Johnsen, *Clim. Dyn.* **14**, 73 (1998).
- U. von Grafenstein, H. Erlenkeuser, A. Brauer, J. Jouzel, S. J. Johnsen, *Science* **284**, 1654 (1999).
- A. Korhola, J. Weckstrom, *Quat. Res.* **54**, 284 (2000).
- A. Nesje, S. O. Dahl, *J. Quat. Sci.* **16**, 155 (2001).
- F. McDermott, D. P. Matney, C. Hawkesworth, *Science* **294**, 1328 (2001).
- For U-Th data [supplement to (10)], see [www.sciencemag.org/cgi/content/full/294/5545/1328/DC1](http://www.sciencemag.org/cgi/content/full/294/5545/1328/DC1).
- I. D. Campbell, C. Campbell, M. J. Apps, N. W. Rutter, A. B. G. Bush, *Geology* **26**, 471 (1998).
- W. E. Dean, *Geol. Soc. Am. Spec. Pap.* **276**, 135 (1993).
- F. S. Hu, H. E. Wright, E. Ito, K. Lease, *Nature* **400**, 437 (1999).
- F. A. Street-Perrott, R. A. Perrott, *Nature* **358**, 607 (1990).
- K. Hugen, J. T. Overpeck, L. C. Peterson, S. Trumbore, *Nature* **380**, 51 (1996).
- R. B. Alley *et al.*, *Geology* **25**, 483 (1997).
- T. Blunier, J. Chappellaz, J. Schwander, B. Stauffer, D. Raynaud, *Nature* **274**, 46 (1995).
- D. C. Barber *et al.*, *Nature* **400**, 344 (1999).
- H. Renssen, H. Goosse, T. Fichefet, J.-M. Campin, *Geophys. Res. Lett.* **28**, 1567 (2001).
- Stalagmite CC3 was chosen because of its location on the North Atlantic margin and because previous work detected the 8200-year event as the only high-amplitude O isotope excursion during the entire Holocene (10, 11).
- M. S. Roberts, P. L. Smart, A. Baker, *Earth Planet. Sci. Lett.* **154**, 237 (1998).
- I. J. Fairchild *et al.*, *Chem. Geol.* **166**, 255 (2000).
- I. J. Fairchild *et al.*, *J. Geol. Soc.* **158**, 831 (2001).
- D. Genty, Y. Quinif, *J. Sediment. Res.* **66**, 275 (1996).
- Y. Huang *et al.*, *Chem. Geol.* **175**, 429 (2001).
- J. Mayer, *J. Cave Karst Stud.* **61**, 131 (1999).
- Elemental concentrations were analyzed with a CAMECA ims-4f ion microprobe at the Department of Geology and Geophysics, University of Edinburgh. The primary ion beam excavates pits to a depth of 2 to 5  $\mu\text{m}$  (41). Each analyzed spot (diameter 10  $\mu\text{m}$ ) was ablated for 15 s before data acquisition to eliminate surface contamination. Si was used to monitor silicate detritus, and data points with Si concentrations greater than 60 ppm and trace element concentrations more than 15% above a 19-point moving average baseline were excluded. Because the bedrock above Crag Cave is a rather pure limestone, Mg does not exhibit any structure and is therefore not discussed. The factors controlling H are poorly understood, and it exhibits no systematic trends. The age of the calcite at the beginning and end of the 7762- $\mu\text{m}$  track, determined by linear interpolation between U-Th-dated points (10, 11), corresponds to  $8260 \pm 80$  years B.P. and  $8370 \pm 80$  years B.P., respectively. Several shorter ancillary tracks parallel to and overlapping the principal track (Fig. 1) confirmed the reproducibility of data. The principal track consists of 1018 data points, corresponding to an actual mean spacing of 7.3  $\mu\text{m}$ , implying an average spot overlap of 27%.
- R. B. Lorenz, *Geochim. Cosmochim. Acta* **45**, 553 (1981).
- Y. Huang, I. J. Fairchild, *Geochim. Cosmochim. Acta* **65**, 46 (2001).
- Slow, near-equilibrium calcite deposition typically results in optically clear calcite with few inclusions, which is characteristic of the calcite deposited during the first-order shift. A simultaneous decrease in inferred U-Th growth rates (10, 11) and growth rates reconstructed by counting trace element cycles within the calcite (discussed in the text) corroborates the contention that the clear calcite within the event was the result of slow, near-equilibrium deposition.
- A. Ayalon, M. Bar-Matthews, A. Kaufman, *The Holocene* **9**, 715 (1999).
- A. A. Finch, P. A. Shaw, G. P. Weedon, K. Holmgren, *Earth Planet. Sci. Lett.* **186**, 255 (2001).
- Mean amplitude was quantified by calculating the standard deviation of the detrended subsets (before, during, and after the event) of the data.
- D. Genty, A. Baker, B. Vokal, *Chem. Geol.* **176**, 191 (2001).
- R. B. Alley *et al.*, *Nature* **362**, 527 (1993).
- M. Stuiver, P. M. Grootes, T. F. Braziunas, *Quat. Res.* **44**, 341 (1995).
- A. Baker, P. L. Smart, D. C. Ford, *Palaeogeogr. Palaeoclimatol. Palaeoecol.* **100**, 291 (1993).
- D. Genty, Y. Quinif, *J. Sediment. Geol.* **66**, 275 (1996).
- A. Schmittner, M. Yoshimori, A. J. Weaver, *Science* **295**, 1489 (2002).
- R. W. Hinton, in *Microprobe Techniques in the Earth Sciences*, P. J. Potts, J. F. W. Bowles, S. J. B. Reed, M. R. Cave, Eds. (Chapman, London, 1995), pp. 235–289.
- We gratefully acknowledge the assistance of R. Hinton and J. Craven with the ion microprobe at the University of Edinburgh. We thank the owners of Crag Cave for their continued cooperation and enthusiasm. We thank two anonymous reviewers for their constructive reviews. Supported by Enterprise Ireland grant SC/1999/012/.

12 March 2002; accepted 1 May 2002

## Insights into Collisional Magmatism from Isotopic Fingerprints of Melting Reactions

Kurt M. Knesel<sup>1\*</sup> and Jon P. Davidson<sup>2</sup>

Piston-cylinder experiments in the granite system demonstrate that a variety of isotopically distinct melts can arise from progressive melting of a single source. The relation between the isotopic composition of Sr and the stoichiometry of the observed melting reactions suggests that isotopic signatures of anatectic magmas can be used to infer melting reactions in natural systems. Our results also indicate that distinct episodes of dehydration and fluid-fluxed melting of a single, metapelitic source region may have contributed to the bimodal geochemistry of crustally derived leucogranites of the Himalayan orogen.

The isotopic characteristics of melt and restite during anatexis have not been studied in detail in controlled laboratory experiments. It is assumed that the isotopic compositions of melts are given by the bulk composition of the protolith—an assumption that implies isotopic equilibration is attained between the melt and source minerals. Recent observations have called this assumption into question at shallow crustal pressures (1–3), leading us to extend the question to deeper levels in the crust. Here we report experimental results on dehydration melting involving both muscovite and biotite and show how the results can be used to infer melting reactions involved in the petrogenesis of crustally derived granites of the Himalayan orogen. Such information is useful for understanding the role of fluids and the influence of deformation on anatectic melting during collisional orogenesis.

Experiments were performed at 600 MPa and 850 to 1000°C in a piston-cylinder appara-

tus with the use of a diamond-aggregate extraction technique (4). In a melt-extraction experiment, a thin layer of ~50- $\mu\text{m}$ -sized diamonds is loaded on top of ~300 mg of 75- to 100- $\mu\text{m}$ -sized grains of crushed granite in a graphite cylinder housed in a large-volume, thick-walled Ni capsule (5). The use of crushed granite rather than a fine powder or gel is a unique and important aspect of the experimental design because it allows us to simulate the influence of minerals on isotopic variations during melting. When brought to run conditions (6), partial melt from the crushed granite is driven into pore space in the overlying diamond powder by the transient pressure gradient between the two layers. At the end of the experiment, quenched melt (glass) in the diamond layer is separated from the residual silicate (crushed granite) by sectioning with a diamond wafer saw. The glass is dissolved away from the diamond, and the Sr-isotopic compositions in the glass are measured by thermal ionization mass spectrometry (7).

Variation of <sup>87</sup>Sr/<sup>86</sup>Sr ratios of experimental melts as a function of the duration of the experiment shows that, for short durations, the isotopic composition of the melt is distinct from that of the bulk starting assemblage (Fig. 1). However, the <sup>87</sup>Sr/<sup>86</sup>Sr of the melt approaches that of

<sup>1</sup>Department of Earth Sciences, University of Queensland, Brisbane, Qld 4072, Australia. <sup>2</sup>Department of Earth Sciences, University of Durham, Durham, DH1 3LE, UK.

\*To whom correspondence should be addressed. E-mail: k.knesel@earth.uq.edu.au

the initial crushed granite with increasing time. These results confirm that melt in the diamond layer remains chemically connected with the residual mineral assemblage via a network of melt along grain boundaries. This network, which is verified by petrographic inspection, serves as a diffusive pathway between the two reservoirs.

The variation of  $^{87}\text{Sr}/^{86}\text{Sr}$  ratios in the experimental melts, extrapolated to the onset of melting as a function of temperature, shows a range of values dependent on the mineral phases involved in the melting process (Table 1). At 850°C, the  $^{87}\text{Sr}/^{86}\text{Sr}$  of the melt is lower than the bulk crushed granite because of the high concentration of relatively unradiogenic Sr in the plagioclase consumed during dehydration melting of muscovite. With increasing temperature, the  $^{87}\text{Sr}/^{86}\text{Sr}$  ratio of the melt increases monotonically, though a step-wise increase is suggested above 950°C due to the increased melting and dissolution of biotite. This trend is consistent with experimental observations on melting relations of metapelitic rocks (8), which show that melting at temperatures higher than those of the muscovite-out boundary is controlled by dissolution of alkali feldspar, followed by incongruent breakdown of biotite. This agreement suggests that, if the mineralogic composition of the protolith and the isotopic compositions of the constituent minerals are known, isotopic compositions of anatectic magmas can be used to infer melting reactions in natural systems.

Before extrapolating our experimental results to natural systems, it is worthwhile to comment on the homogenization of Sr isotopes during crustal melting. The time scales for isotopic equilibration in our experiments range from weeks to months (Fig. 1) because of the small grain size (75 to 100  $\mu\text{m}$ ) and relatively high temperatures (850 to 1000°C) in the experiments. In nature, residual minerals are generally one to two orders of magnitude larger than in

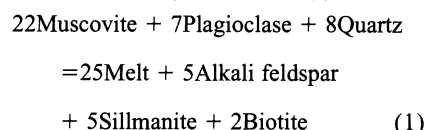
our experiments and anatectic temperatures may be as low as 700°C. Time scales of equilibration by diffusion are, therefore, protracted in the continental crust and are of the order  $\sim 10^6$  years for typical synorogenic anatectic conditions (1). Given that low melt-fraction liquids may be extracted at rates as high as 2 m year<sup>-1</sup> (9) over time scales as brief as 10 to 100 years (10), melt-source equilibration may not be attained before final extraction and ascent of granitic magma in the continental crust.

Our experiments differ further from anatexis in nature in that the source rock was heated to melting temperatures in a matter of minutes, thus ensuring preservation of isotopic differences among constituent minerals at the onset of melting. Theoretical considerations suggest that such heterogeneity may not survive prograde heating during collisional orogenesis (11), because the time scales for thermal relaxation after crustal thickening are longer ( $>10^6$  year) than those required to achieve isotopic homogenization by volume diffusion. Yet, recent studies of migmatites in the Hercynian anatectic complex of Toledo, Spain (12), and of pelitic gneisses of the Nanga Parbat-Haramosh massif in the western Himalaya (13) show that Sr-isotopic heterogeneity can be preserved on the mineralogic scale before and during anatexis in some orogenic terrains. Such disequilibrium may require rapid heating due to an external heat source, such as shear heating on major crustal shear zones (14) or input of mantle-derived heat (15); it could also suggest that isotopic homogenization may not be related to temperature through diffusion alone. Homogenization may instead be governed by complex factors that may vary even within a given sample, such as the degree and distribution of recrystallization and shearing, the nature of fluid flow, and the original mineralogic composition and textural characteristics of the protolith (13). In short, isotopic homogenization is not a ubiquitous consequence

of prograde metamorphism preceding anatexis, and the consequences of isotopic redistribution on anatexis are, therefore, well worth examining.

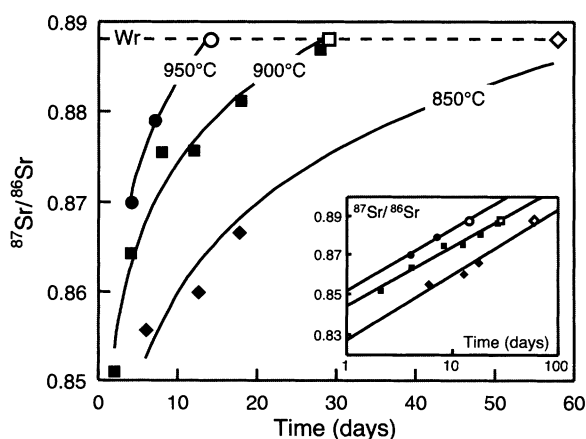
We used experimental constraints on melting reactions of likely protoliths (8) and our experimental data to model isotopic compositions of melts parental to leucogranites of the Himalayan orogen, some of the best-known examples of pure crustal melts (16). A striking feature of these granites is their bimodal isotopic and trace element geochemistry (14, 17), perhaps best exemplified by the well-studied Manaslu intrusive complex (Fig. 2). This heterogeneity has been attributed to mixing between two source components, delimited by metapelitic and metagreywacke end members (14, 17). We propose an alternative model whereby differences in the nature and, therefore, the stoichiometry of melting reactions give rise to variations in Sr-isotopic compositions of granitic melts from a single metapelitic source, as we have shown in our experiments.

A growing consensus has emerged that recognizes the leucogranites of the high Himalaya were generated by dehydration melting of muscovite-bearing metasediments (18). These melts may be expressed by the reaction (8)



Using a typical kyanite-grade, two-mica schist from the high Himalayan crystalline series (8) as a model protolith, we find muscovite-dehydration melting by reaction 1 produces liquid with an  $^{87}\text{Sr}/^{86}\text{Sr}$  ratio less than the source rock (Fig. 2; solid circles), near the average value for the relatively low Sr [ $<65$

**Fig. 1.** Results of experiments performed at 600 MPa and 850°C (diamonds), 900°C (squares), and 950°C (circles). Starting materials comprised 14 wt. % biotite (30 ppm Sr), 3 wt. % muscovite (41 ppm Sr), 26 wt. % alkali feldspar (135 ppm Sr), 27 wt. % plagioclase (288 ppm Sr), and 30 wt. % quartz. The isotopic compositions of the starting materials are reported in Table 1. Open symbols show approximate times for melts to attain isotopic equilibrium with the source rock (dashed line labeled Wr) based on exchange with residual biotite, assuming kinetic data for Sr diffusion in (27) and the simple relation  $t = a^2/D$ .

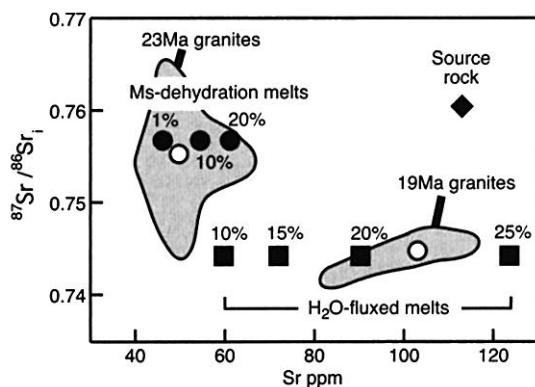


Agreement between power-law fits to the time series data and calculated equilibrium results confirms that segregated melt remains chemically connected to the underlying residual silicate. Experiments at 1000°C are not shown because they plot above the whole-rock composition, due to the large contribution of radiogenic Sr from biotite. Inset shows regression of time series data used to extrapolate initial melt compositions in Table 1.

**Table 1.**  $^{87}\text{Sr}/^{86}\text{Sr}$  ratios of starting materials and experimental melts extrapolated to the beginning of melting by least-squares regression of time series data ( $\pm 1\sigma$ ). The isotopic composition of the bulk starting material (whole rock) represents the mean ( $\pm 1\sigma$ ) of three dissolutions of 300 mg of the crushed granite. The isotopic ratios of the mineral phases in the crushed granite are from (2). Analytical uncertainties ( $2\sigma$  SD) of measured ratios reflect the long-term reproducibility of SRM 987 (7), except for biotite, where the within-run standard error is reported.

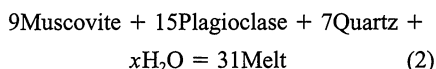
Temp. (°C)/ phase	$^{87}\text{Sr}/^{86}\text{Sr}$	Error
<i>Extrapolated (initial) melt compositions</i>		
850	0.827	0.003
900	0.845	0.002
950	0.851	0.003
1000	0.938	0.005
<i>Starting materials (crushed granite)</i>		
Whole rock	0.8884	0.0002
Plagioclase	0.79065	0.00002
Alkali feldspar	0.89082	0.00002
Muscovite	0.97507	0.00002
Biotite	3.4293	0.0003

**Fig. 2.** Comparison of Sr-isotope compositions of dehydration and H<sub>2</sub>O-fluxed melts with leucogranites from the Manaslu intrusive complex (Nepalese Himalaya) for which monazite crystallization ages have been determined by Th-Pb ion probe dating (14). Leucogranites (outlined fields) are grouped into low-Sr (≤65 ppm) and high-Sr (≥80 ppm) fields dated at 23 and 19 Ma, respectively. The average composition of each episode of magmatism is denoted by an open circle. Isotopic ratios of plagioclase and muscovite used in melting models represent <sup>87</sup>Sr/<sup>86</sup>Sr calculated at 23 and 19 Ma (28). Muscovite-dehydration melting at 23 Ma produces melts (solid circles) with <sup>87</sup>Sr/<sup>86</sup>Sr ratios less than schistose source rock (solid diamond) and Sr concentrations (29) spanning the low-Sr field at low to moderate melt fractions. Melt fraction is labeled in %. Water-fluxed melting at 19 Ma yields lower <sup>87</sup>Sr/<sup>86</sup>Sr liquids (solid squares), which span the high-Sr field at relatively high melt fractions.



parts per million (ppm)] Manaslu granites (Fig. 2; open circle). Though our experiments support this result (Table 1), we note that the calculated melt compositions represent hypothetical end members given that individual minerals would have been partially reset before anatexis, albeit to an unknown extent.

Although it accounts adequately for the high-<sup>87</sup>Sr/<sup>86</sup>Sr, low-Sr granites (Fig. 2), muscovite-dehydration melting of a pelitic source cannot account for production of the granites with relatively high Sr concentrations (>80 ppm) and low <sup>87</sup>Sr/<sup>86</sup>Sr ratios. In contrast, H<sub>2</sub>O-fluxed melting, which may be expressed by the reaction (8)



where *x* is the stoichiometric coefficient for H<sub>2</sub>O added to the experiment, consumes plagioclase in greater proportion than muscovite, and therefore produces higher Sr melts with <sup>87</sup>Sr/<sup>86</sup>Sr ratios lower than muscovite-dehydration melting (Fig. 2; solid squares). This result alleviates the need to invoke a different source composition to account for the Sr-isotope signatures of the relatively high-Sr granites and provides support for a role for water in the generation of some Himalaya leucogranites (19). Moderately high melt fractions [~20 to 25 weight percent (wt. %)] are required to yield appropriate trace-element concentrations (Fig. 2), which is consistent with experimental constraints indicating that hydrous melting at mid-crustal depths generates granitic compositions only if melt fractions are high enough to require substantial breakdown of muscovite (8). At low melt fractions (≤10 wt. %), H<sub>2</sub>O-fluxed melts are trondhjemitic.

Disequilibrium compositions, such as those proposed here, may be an inevitable result of rapid production, extraction, and ascent of anatectic melt in dynamic orogenic environments (10). During Himalayan anatexis, shear-

enhanced compaction (20) as well as feedback mechanisms between melting and deformation (21) may have promoted rapid extraction of anatectic liquids at low to moderate melt fractions, thereby arresting isotopic exchange between melt and source before complete equilibration. The melt residence times calculated from accessory-phase dissolution rates, which indicate that some Himalayan leucogranites may have been extracted in less than 7 thousand years (ky) (22), support this suggestion. For anhydrous conditions, high dilational strain generated by muscovite-dehydration melting (23) may have further encouraged melt segregation. In contrast, reduction in volume during hydrous melting may hinder complete extraction (24), thereby favoring isotopic equilibration of the residual melt fraction. Inasmuch as hydrous melting may lead to migmatitic structure, apparent Sr-isotopic homogenization of an anatectic migmatite from the Zaskar Himalaya (11) supports this scenario.

**References and Notes**

1. T. Hammouda, M. Pichavant, M. Chaussidon, *Earth Planet. Sci. Lett.* **144**, 109 (1996).
2. K. M. Knesel, J. P. Davidson, *Geology* **24**, 243 (1996).
3. S. Tommasini, G. R. Davies, *Earth Planet. Sci. Lett.* **148**, 273 (1997).
4. M. B. Baker, E. M. Stolper, *Geochim. Cosmochim. Acta* **58**, 2811 (1994).
5. J. C. Ayers, J. B. Brenan, B. E. Watson, D. A. Wark, W. G. Minarik, *Am. Mineral.* **77**, 1080 (1992).
6. Experiments were carried out in 2.54-cm, NaCl-graphite furnace assemblies. At or above 900°C, graphite furnaces were isolated from the salt pressure-transmitting medium by a Pyrex sleeve. Temperature was measured using Pt-PtRh thermocouples. Uncertainties in temperature measurements were not determined. However, double-thermocouple experiments (5) indicate that the high thermal conductivity of Ni capsules of the same dimensions used here reduces the thermal gradient to ~5°C over a sample length of 8 mm at 10 kbar and 1000°C. As a conservative measure, uncertainties in temperature are taken as ±10°C.
7. Glass was dissolved in a warm 50:50 Hf-H<sub>2</sub>O mixture in sealed Teflon beakers for 4 hours. The mixture was spun with a centrifuge, and the acid containing the dissolved glass was removed by pipette and dried in preparation for cation-exchange chemistry. Leaching tests indicate that the diamond powder contributes less than 0.15% to the total Sr analyzed. The isotopic compositions of the

experimental glasses were measured on a VG sector mass spectrometer following procedures outlined in earlier work (25). Repeated analysis of the Sr standard SRM 987 over the study period yielded a value of 0.710227 ± 25 (2σ SD, *n* = 22 analyses).

8. A. E. Patiño Douce, H. Harris, *J. Petrol.* **39**, 689 (1998).
9. N. Petford, *J. Geophys. Res.* **100**, 15735 (1995).
10. E. W. Sawyer, *J. Petrol.* **32**, 701 (1991).
11. N. Harris, M. Ayres, *J. Geol. Soc. London Spec. Publ.* **738** (1998), p. 171.
12. L. Barbero, C. Villaseca, G. Rogers, P. E. Brown, *J. Geophys. Res.* **100**, 15745 (1995).
13. M. T. George, J. M. Bartlett, *Tectonophysics* **260**, 167 (1996).
14. T. M. Harrison *et al.* *J. Petrol.* **40**, 3 (1998).
15. N. Petford, K. Gallagher, *Earth Planet. Sci. Lett.* **193**, 483 (2001).
16. C. France-Lanford, P. Lefort, *J. Trans. R. Soc. Edinburgh Earth Sci.* **79**, 183 (1988).
17. S. Guillot, P. Le Fort, *Lithos* **35**, 221 (1995).
18. N. Harris, M. Ayres, J. Massey, *J. Geophys. Res.* **100**, 15767 (1995).
19. P. Le Fort, *J. Geophys. Res.* **86**, 10545 (1981).
20. E. H. Rutter, D. H. K. Neumann, *J. Geophys. Res.* **100**, 15697 (1995).
21. R. S. D'Lemos, M. Brown, R. A. Strachan, *J. Geol. Soc. London* **149**, 487 (1992).
22. M. Ayres, N. Harris, D. Vance, *Mineral. Mag.* **61**, 29 (1997).
23. T. Rushmer, *J. Trans. R. Soc. Edinburgh Earth Sci.* **87**, 73 (1996).
24. M. Brown, Y. A. Averkin, E. L. McLellan, *J. Geophys. Res.* **100**, 15655 (1995).
25. K. M. Knesel, J. P. Davidson, *Contrib. Mineral. Petrol.* **136**, 285 (1999).
26. J. Hertogen, R. Gijbels, *Geochim. Cosmochim. Acta* **40**, 313 (1976).
27. C.-H. Chen, D. J. DePaolo, C.-Y. Lan, *Earth Planet. Sci. Lett.* **143**, 125 (1996).
28. The source rock used in the melting models is a kyanite-grade, two-mica schist [sample PAN-3 of (11)], which was studied experimentally (8) to constrain phase relations during melting of likely sources of Himalayan leucogranites. The schist (15 ppm Sr; <sup>87</sup>Sr/<sup>86</sup>Sr<sub>23Ma</sub> = 0.7606, 0.7609) consists of 29% muscovite (128 ppm Sr; <sup>87</sup>Sr/<sup>86</sup>Sr<sub>23Ma</sub> = 0.7722, 0.7726), 11% plagioclase (An<sub>28</sub>; 321 ppm Sr; <sup>87</sup>Sr/<sup>86</sup>Sr<sub>23Ma</sub> = 0.7376, 0.7377), 38% quartz, 13% biotite, 6% garnet, and 4% kyanite+staurolite+tourmaline. <sup>87</sup>Sr/<sup>86</sup>Sr ratios were calculated at 23 and 19 million years ago (Ma) for muscovite-dehydration and fluid-fluxed melting, respectively, assuming bulk-rock homogenization at 500 Ma as reported in (11).
29. The concentration of Sr in anatectic melt was modeled by the following expression for nonmodal, fractional melting

$$\frac{C_L}{C_0} = \frac{1}{D} \left( 1 - \frac{PF}{D} \right)^{\left( \frac{1}{P} - 1 \right)}$$

where *C*<sub>0</sub> is the concentration in the initial solid, *C*<sub>L</sub> is the concentration in the liquid, *D*<sub>0</sub> is the bulk solid-liquid distribution coefficient weighted according to the modal assemblage in the source, *F* is the degree of melting, and *P* is the bulk distribution coefficient weighted according to the proportion of phases entering the melt. The effect of product mineral growth on melt chemistry during incongruent breakdown of muscovite was accounted for by replacement of *P* in the equation above with *Q* (26)

$$Q = \frac{p - p^\alpha \sum_i t_i k_i'}{1 - p^\alpha (1 - t)}$$

where *p*<sub>*i*</sub> is the mass contribution of phase *i* to the liquid, *t*<sub>*i*</sub> is the mass fraction of the incongruent phase contributed to the liquid and product mineral phases. Sr-partition coefficients are given in (18).

30. We thank C. Manning and R. Newton for guidance in the piston-cylinder laboratory at the University of California at Los Angeles and the journal reviewers for their helpful comments. Supported by the NSF.

6 February 2002; accepted 27 April 2002